

Mountain permafrost and energy balance on Juvvasshøe, southern Norway

K. Isaksen* & E.S.F. Heggem†

*Norwegian Meteorological Institute, Oslo, Norway

S. Bakkehøi

The Norwegian Geotechnical Institute, Oslo, Norway

R.S. Ødegård

Gjøvik University College, Gjøvik, Norway

T. Eiken†, B. Etzelmüller† & J.L. Sollid†

†Department of Physical Geography, University of Oslo, Oslo, Norway

ABSTRACT: Ground temperatures and near surface energy fluxes are measured and modelled for the years 2000 and 2001 at a high mountain site, Juvvasshøe (1894 m a.s.l.), Jotunheimen, southern Norway. The results show a high correlation between air-, ground surface- and ground temperatures. The small thermal offset suggests a strong coupling between microclimate and the ground thermal regime. The close relationship between air- and ground temperatures is mainly explained by high turbulent fluxes, good ventilation in the upper surface layers, together with the lack of vegetation, low availability of water and the almost absent snow cover at the study site. Net radiation and sensible heat fluxes are the dominating energy fluxes and give a nearly balanced energy budget.

1 INTRODUCTION

In a mountain permafrost environment, the rugged topography leads to large differences in microclimate. Ground temperatures are highly sensitive to energy exchange between the atmosphere and the ground surface. Previous studies in southern Norway indicate that the lower altitudinal limit of mountain permafrost is correlated to a mean annual air temperature (MAAT) of -2°C or colder (Isaksen et al., 2002; Ødegård et al., 1996). These studies are based on local statistic-empirical models using BTS (Bottom Temperature of Snow) measurements. A generalised regional permafrost model for southern Norway was presented by Etzelmüller et al. (1998). These models connect permafrost existence to air temperature, but do not attempt to model the explicit energy exchange components. Rather few studies focus on the thermal regime within the active layer or on the energy fluxes of mountain permafrost (Harris & Pedersen, 1998; Hoelzle et al., 2001; Humlum, 1997; Mittaz et al., 2000). Most investigations of the thermal offset (defined as the difference between mean annual ground temperature at the permafrost table and mean annual ground surface temperature) have been performed in high-latitude lowlands rather than in the mountain environment (cf. Hoelzle et al., 2001).

In this study we present results from Juvvasshøe in Jotunheimen, southern Norway (Fig. 1), which is one of the established PACE (Permafrost and Climate in Europe) drill sites (Sollid et al., 2000). Near surface energy-exchange processes and ground temperatures are calculated and discussed in relationship to surface

characteristics. The aim is to get a detailed knowledge of all the energy balance components involved, and to understand how they are linked to mountain permafrost.

2 FIELD SITE AND METHODS

Juvvasshøe is a small mountaintop located at the rim of a 4 km^2 mountain plateau (Juvflya) in Jotunheimen, southern Norway (Fig. 1).

The bedrock on Juvvasshøe consists of crystalline rocks comprised of mainly quartz monzonite (Kvartsjotunitt). The vegetation cover is sparse and limited to black lichen. The boulder surface (block field) consists mainly of weathered detritus material, generally 3–5 metres thick (Fig. 2).

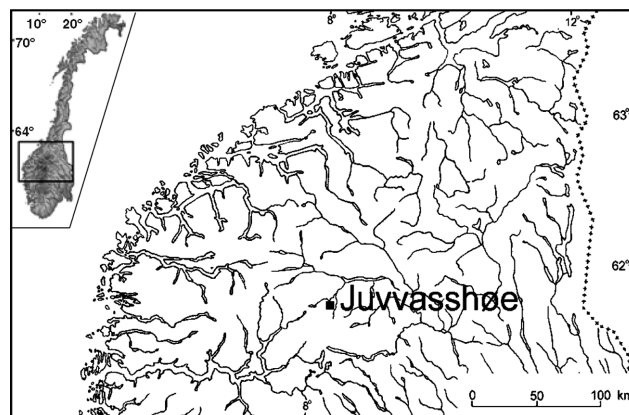


Figure 1. Location of Juvvasshøe (1894 m a.s.l., $61^{\circ} 40' 32''\text{N}$, $8^{\circ} 22' 04''\text{E}$) in Jotunheimen, southern Norway.

Mean annual air temperatures (MAAT) on Juvvasshøe in 2000 and 2001 were -3.4°C and -4.3°C , respectively. MAAT for the normal period 1961–1990 is estimated to be $-4.75 \pm 0.25^{\circ}\text{C}$. The lowest air temperature during the two years was -32.4°C (3 Feb. 2001), while the highest was 13.9°C (26 Aug. 2000). The mean wind speed was 6.3 m s^{-1} , with a maximum of 27.9 m s^{-1} (7 Jan. 2000). Prevailing

winds were from the south and west. Field observation reveals that the strong winds result in a scarce snow cover until March and April, with a maximum of less than 0.2 m in April. The average annual precipitation according to Østrem et al. (1988) is 800 mm. For other mean values, see Table 1.

Ground temperature measurements in a 10 m deep borehole at Juvflya, nearby Juvvasshøe, were initiated in 1982 by Ødegård et al. (1992). The drilling of a 129 m deep borehole at Juvvasshøe was completed on 4 August 1999 (Isaksen et al., 2001; Sollid et al., 2000). Borehole casing, sensors, depth of thermistors and data logging equipment were assembled according to guidelines provided by the PACE-project in order to optimise comparability and standardise procedures between sites (Harris et al., 2001). To stabilise the borehole within the surface layers, the upper 3.5 m was cased with concrete. To control the thermal influence of the concrete and to get a better resolution of the annual variations, a 20 m deep borehole (without concrete) was drilled 17 m away. Ground temperature data used in this paper is obtained from 17 thermistors (NTC) in the 20 m deep control borehole. The measurement interval is six hours. Ground surface temperatures at 0.1 m depth were measured with three miniature-temperature loggers (UTL-1, TMC-1T thermistors), reading the temperature every second hour. Ground structure and stratigraphy achieved during and after drilling are described in Figure 2.

In September 1999 an automatic micrometeorological station was established three metres from the main borehole, measuring in and outgoing short and long wave radiation, air temperature, humidity, and wind speed and direction. None of the radiation sensors are heated. The station has a 2 m anemometer height and measurement interval is according to standard meteorological observations for automatic stations, with data storage every hour. Data collected from the borehole, UTL1 miniature loggers and climate station were used as input for modelling the energy-exchange fluxes between the atmosphere and the ground. Because of instrument failure, radiation data from May to July and December 2001 are not available. Methods and parameterisation for the energy balance are summarised in Table 2.

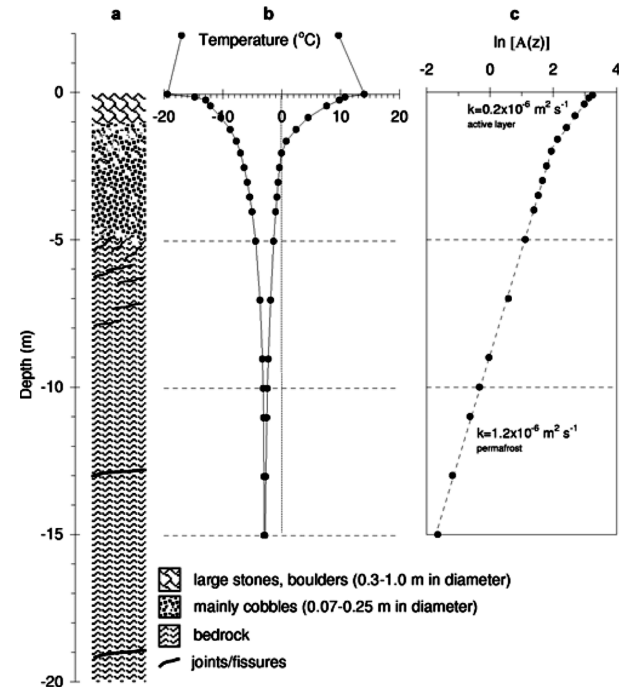


Figure 2. Principal results from temperature measurements and geophysics in a 20 m deep borehole at Juvvasshøe. (a) The stratigraphy of the borehole is characterised by frost sorting in the surface layers. Juvvasshøe is mantled by weathered mountaintop detritus material (blockfield), with surface boulders generally up to one meter in size. Below the first meter, grain size decreases and the material is dominated by cobbles down to the bedrock at about 5 m depth. (b) The amplitude (air- and ground- maximum and minimum temperatures) of the year 2000 temperature cycle plotted against depth. Note the distinct damping of the thermal amplitude within the active layer (2.0 m). Zero annual amplitude depth is 16 m. The absolute accuracy for the borehole-temperature measurements is $\pm 0.05^{\circ}\text{C}$ and the relative accuracy at $\pm 0.02^{\circ}\text{C}$. (c) The natural logarithm of the maximum amplitude of annual fluctuations vs. depth. See text for details.

Table 1. Mean values for temperatures and energy fluxes for years 2000 and 2001. Temperatures: T_A = air (2 m), T_S = estimates at surface, $T_{0.1\text{m}}$ = 0.1 m (from UTL miniature temperature logger), $T_{0.2\text{m}}$ = 0.2 m, $T_{2.0\text{m}}$ = 2.0 m and $T_{15.0\text{m}}$ = 15.0 m. ΔT is thermal offset. Q_H , Q_G , $S\uparrow$, $S\downarrow$, $L\uparrow$ and $L\downarrow$ are energy fluxes. Wind = wind speed, RH = relative humidity and Q^* = sum of all estimated energy fluxes.

Year	T_A $^{\circ}\text{C}$	T_S $^{\circ}\text{C}$	$T_{0.1\text{m}}$ $^{\circ}\text{C}$	$T_{0.2\text{m}}$ $^{\circ}\text{C}$	$T_{2.0\text{m}}$ $^{\circ}\text{C}$	$T_{15.0\text{m}}$ $^{\circ}\text{C}$	ΔT $^{\circ}\text{C}$	Q_H Wm^{-2}	Q_G Wm^{-2}	$S\uparrow$ Wm^{-2}	$S\downarrow$ Wm^{-2}	$L\uparrow$ Wm^{-2}	$L\downarrow$ Wm^{-2}	Wind ms^{-1}	RH %	Q^* Wm^{-2}
2000	-3.4	-2.7	-2.4	-2.1	-2.5	-2.9	0.1	-34.2	-3.5	38	122	300	261	6.8	83	7.8
2001	-4.3		-3.7	-3.0	-2.9	-2.9	-0.8							5.7	80	

Table 2. Energy balance components: Radiation: $S\downarrow$, $S\uparrow$ are incoming and outgoing shortwave radiation, $L\downarrow$, $L\uparrow$ are incoming and outgoing longwave radiation. Turbulent fluxes: ρ is air density, C_p is specific heat of air, k is von Karman's constant, $z_u z_t$ is surface roughness length for wind-speed and temperature. Surface roughness length was set to 0.05 m during snow-free conditions due to the block-size, and 0.01 m for snow covered ground (assume a mixture of snow and rocks), since no wind profile data exist at the site. Δu , $\Delta \theta$ are differences in wind-speed and temperature between surface and measurement level, $\Delta z_{u,t}$ is the log mean height measure level. $\phi_{m,x}$ are Monin-Obukhov functions. Ground heat flux: k is thermal conductivity of the ground, here selected to $3.3 \text{ W m}^{-1} \text{ K}^{-1}$ for Juvvasshøe (Isaksen et al., 2001), $\Delta t, z$ are the temperature and height difference between the thermistors at 0.2 m and 0.4 m. Surface characteristics: α is the surface albedo, ε is ground emissivity. $L\uparrow (0^\circ\text{C})$ is outgoing longwave radiation at 0°C and σ is the Stefan-Boltzmann constant. Snow emissivity is assumed constant at all times,

Parameters	Modelling	Comments
Short- and long-wave radiation	$S\downarrow$, $S\uparrow$, $L\downarrow$, $L\uparrow$, measured directly	$S\downarrow$ values were adjusted due to a calibration problem in sensor.
Sensible heat flux	$Q_H = -\rho C_p k^2 z_u z_t ((\Delta u \Delta \theta) / (\Delta z_u \Delta z_t)) (\Phi_m \Phi_x)^{-1}$	Bulk method, (Oke, 1987)
Latent heat flux	$Q_{LE} = 0$	Not estimated
Ground heat flux	$Q_G = -k(\Delta t / \Delta z)$, pure heat conduction	Used the two uppermost thermistors in borehole
Heat flux trough snow cover	$Q_S = \text{not estimated}$	Thin, well packed snow cover without any insulating effects
Snowmelt energy	$Q_M = 0$	Not estimated.
Albedo	$\alpha = S\uparrow / S\downarrow$, Adjusted $S\downarrow$ was used	Estimated each day at 11 GMT to avoid errors due to low solar height.
Ground emissivity	$\varepsilon = L\uparrow (0^\circ\text{C}) / (\sigma 273.15 \text{ K}^4)$, gave $\varepsilon = 0.99$	Assuming 0°C during the zero curtain effect period in spring.
Snow emissivity	$\varepsilon_{\text{snow}} = 0.98$	Assumed. Oke (1987) suggest [0.82–0.99]

3 RESULTS AND INTERPRETATIONS

3.1 Ground temperatures and thermal diffusivities

The calculated mean ground surface temperature (MGST) in 2000 was -2.7°C , which is 0.7°C higher than the MAT. For 2000 and 2001 measured mean ground temperatures (MGT) at 0.1 m depth were -2.4°C and -3.7°C ; mean ground temperatures at permafrost table (MGPT) were -2.5°C and -2.9°C , respectively (Table 1). For 2000 the amplitude of the annual temperature cycle (AATC) at the ground surface (0.1 m depth) was 25.5°C , while AATC at the permafrost table was 7.0°C (Fig. 2). Zero annual amplitude (ZAA, $A(z) < 0.1^\circ\text{C}$) occurred at 16 m depth. Mean thermal conductivity in the bedrock is $3.3 \pm 0.3 \text{ W m}^{-1} \text{ K}^{-1}$ (Isaksen et al., 2001). Thermal diffusivity (κ) within the layer of seasonal variations was determined from the amplitude reduction at depth (Fig. 2) and phase lag increase with depth (Fig. 3). Two distinct layers appear in plotting the natural logarithm of the maximum amplitude against depth ($\ln [A(z)]$) (Fig. 2): (1) the upper 0.1–2.0 m and (2) the lower 2.0–15 m, corresponding to the active layer and the permafrost below, respectively. The mean thermal diffusivity for each layer was determined from the slope of the linear fit to $\ln [A(z)]$ (e.g. Vonder Mühll & Haeberli, 1990; Isaksen et al., 2000), which provide a mean diffusivity of $0.2 \times 10^{-6} \text{ m}^2 \text{ s}^{-1}$ in the active layer and $1.2 \times 10^{-6} \text{ m}^2 \text{ s}^{-1}$ in the permafrost. The latter

value gives a phase speed of the annual wave of $6.9 \times 10^{-7} \text{ m s}^{-1}$, equal to $6.0 \times 10^{-2} \text{ m d}^{-1}$.

Seasonal variations in ground temperature in the upper 15 m are shown in Figure 3. The initiation of the spring ground thaw was in the end of April. Maximum thaw depth was 2.0 m and occurred in early August. Autumn freezing started in early October. Figure 3 indicates the relationship between air and ground temperatures within the active layer. In winter the absent or thin snow cover gives no insulating effect, resulting in fast temperature cooling and high frequency variations. Between 1.5 m and 5 m cobbles dominate with some layers of finer, weathered material. Observations during drilling showed that the layers of fine material contained some ice. A short zero-curtain effect during spring and autumn, however, indicates that the water content is low. During autumn freeze-back at all levels between 2 m and 3 m depth, ground temperatures were within the range of 0 to -0.5°C for about four weeks (Fig. 3).

3.2 Energy balance

All radiation components ($S\downarrow$, $S\uparrow$, $L\downarrow$ and $L\uparrow$) were measured directly. Because of a calibration problem in the upper pyranometer (CM3, measuring incoming shortwave radiation) $S\downarrow$ was adjusted by setting radiation at midnight to zero and interpolating the values according to this adjustment. The corrected values were used further in the analysis.

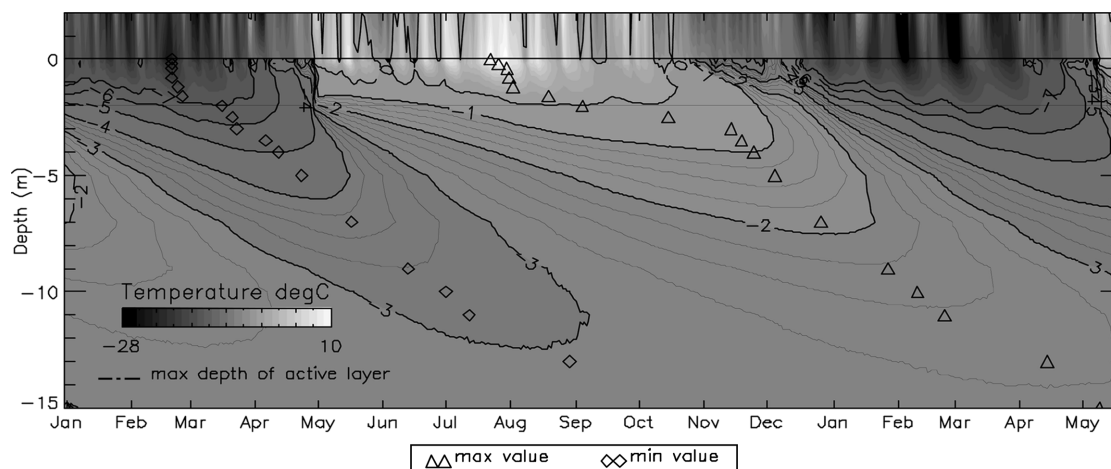


Figure 3. Air temperatures and ground temperatures from 1 Jan. 2000 until 20 May 2001 (each marking indicating the first day of the month), daily average values. Air temperatures at 2 m are obtained from the climate station; surface temperatures from miniature temperature loggers (UTL1) and ground temperatures are taken from the borehole thermistors down to 15 m. The symbols at the plot show the penetration of the maximum- (triangles) and minimum (diamonds) waves of diffusion during the one-year cycle. The sharp gradient at 1 May 2000 and 7 May 2001 are associated with positive air temperatures causing the snow cover to disappear within two days and melt water to penetrate and refreeze in the ground. The figure shows that the thermal diffusivity in the permafrost is nearly equal for both the summer and the winter temperature wave.

Wind speed was measured in one level only. Therefore the bulk method was used for calculating turbulent flux for sensible heat (Q_H). The site is exposed to strong winds during the whole year, leading to high values of Q_H . Turbulent latent heat flux (Q_{LE}) was not calculated since there are no measurements of ground surface humidity. Relative humidity at 2 m was generally high at all times.

Rapid and large drops in temperature and relative humidity occur during winter. During these episodes, which normally last 2–3 days, condensation takes place. In these periods the estimated surface temperature is up to 15°C colder than the measured air temperature. These observations indicate that the not-heated radiation sensors are subject for riming, and cause large errors in several of the energy balance components. The data show one such event in winter 2000 (February) and five in 2001 (January to March). Relative humidity reaches 100% during periods of fog. Such high values might indicate a situation of condensation towards the surface as well as evaporation from it, and thus give a positive component for Q_{LE} .

Ground heat flux (Q_G) was calculated as pure heat conduction through the uppermost part of the ground. Temperature gradient was obtained from the borehole thermistors at 0.2 m and 0.4 m. Q_G remains small during the whole year and is positive during winter and negative in summer.

Since there is no snow depth sensor at the climate station the changes in albedo was used as indication of snow cover. The dark surface at the site gives a sudden drop in the albedo as soon as snow disappears. The albedo is more than 0.5 when snow is present and

about 0.1 during snow free periods. Due to high wind speeds during winter, a snow cover is mostly absent at the site and any remaining snow packs to a dense layer.

Analysis of daily winter values of air temperatures and ground surface temperatures at 0.1 m depth shows little damping of the temperature signal and only one-day delay between air- and ground surface temperatures indicating that the snow cover has little isolating effect and therefore not acts as a buffer layer between the ground and the atmosphere. These observations make calculation of heat flux through snow cover (Q_S) less important at the study site.

Snowmelt (Q_M) estimates is not included in the energy balance since snow-height measurements not exist. This probably influences the energy balance only during the melt periods in April and May.

The radiation components represent the main part of the measured energy budget over the year. During summer the low reflection from the dark surface is compensated by high turbulent fluxes (Q_H) removing energy from the warm surface. The main deviation of the energy budget occurs during spring and autumn, connected to onset of thawing and freezing of the active layer (Figs 3, 5). Closer analyses of daily values show that during May and September 2000 the major modelling problem occurs when the air temperature rapidly fluctuates around 0°C. In these periods especially ground surface temperature seems to be insufficient modelled, leading to large Q_H values and with that, large deviations for the energy budget. The unmeasured Q_M and Q_{LE} probably also have an influence in these periods. The same situation occurs in 2001, only some weeks later.

4 DISCUSSION

The results from the energy balance show that the net radiation and the sensible heat fluxes together give an almost balanced energy budget. Despite neglecting several fluxes in the estimates, the components that were used equal a near-zero energy budget at monthly basis. Furthermore, this site is not likely to be influenced by lateral energy fluxes in the ground, and thereby does not show the problems reported by Mittaz et al. (2000), where the calculated energy budget was non-zero. Since latent heat fluxes and snowmelt energy are not used they probably count for some of the deviation. Parameters as surface emissivity and surface roughness are very sensitive and have great influence on the sensible heat fluxes. These parameters are not measured and will appear as tuning factors in the model. Measurement errors, for instance riming on the sensors, are not excluded from the dataset and will cause large errors and affect the energy balance. Longer data series may give better estimates for these parameters.

In the analyses snow cover measurements were not included. But since the Juvvasshøe station is located at an exposed site, snow cover is generally low during the whole winter. Spatial and seasonal variations of snow cover is important for the presence of permafrost (e.g. Goodrich, 1982; Zhang et al., 2000). Ødegård et al. (1992) measured ground temperatures in a borehole at Juvflya, located 40 m below and 300 m west of Juvvasshøe. At Juvflya the snow depth is larger (0.5–1 m) and ground temperatures at 10 m depth were about 1°C warmer than at Juvvasshøe. Additional investigations around the Juvvasshøe station (Isaksen et al., 2002; King, 1984; Ødegård et al., 1996; Ødegård et al., 1999), show that snow cover can not be neglected in spatial mountain permafrost modelling, as demonstrated by Mittaz et al. (2002).

The results from Juvvasshøe show a close relationship between air- surface and ground temperatures (Figs 3, 4). Thermal offset is less than 1°C. This value seems reasonable due to the low water content and neglectable lateral energy fluxes. This result is in strong contrast with results from the Swiss Alps (Hoelzle et al., 2001; Mittaz et al., 2000) and from Greenland (Humlum, 1997), where thermal offsets of more than 5°C have been observed.

The surface characteristics, bedrock lithology and diffusivity results on Juvvasshøe suggest that permafrost would respond rapidly to climatic variations. The thermal diffusivity values found in the permafrost are typical for bedrock (e.g. Carslaw & Jaeger, 1959) and suggest that the thermal wave (i.e. 5% change) propagates to about 16 m in one year, 50 m in 10 years, 160 m in 100 years and 500 m in 1000 years.

The results of the presented ground temperatures indicate a strong coupling to air temperatures. The

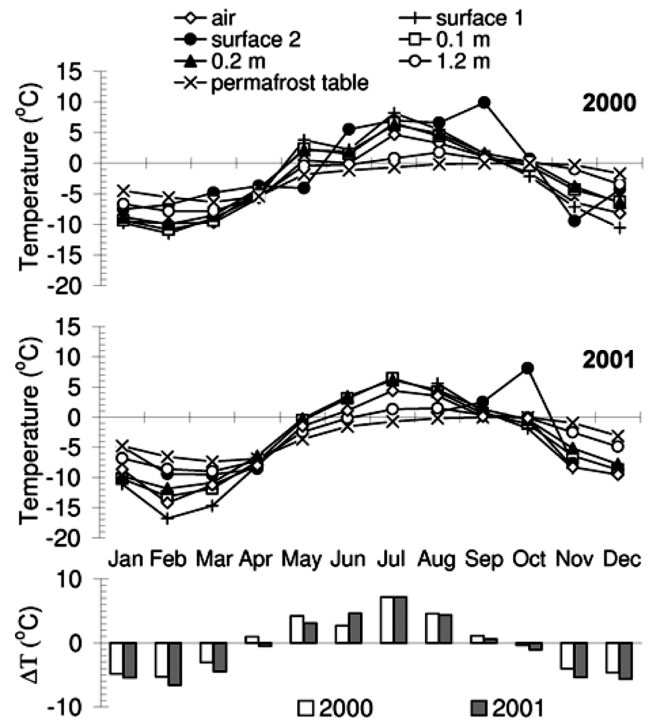


Figure 4. Monthly average air-, surface- (1 – calculated from the sum of all energy fluxes; 2 – calculated from observed $L\uparrow$) 0.1 m depth-, 0.2 m depth-, 1.2 m depth and permafrost table temperatures. Monthly thermal offset (ΔT , e.g. the difference between T_{ps} and T_{gs}) values are shown in the lower graph.

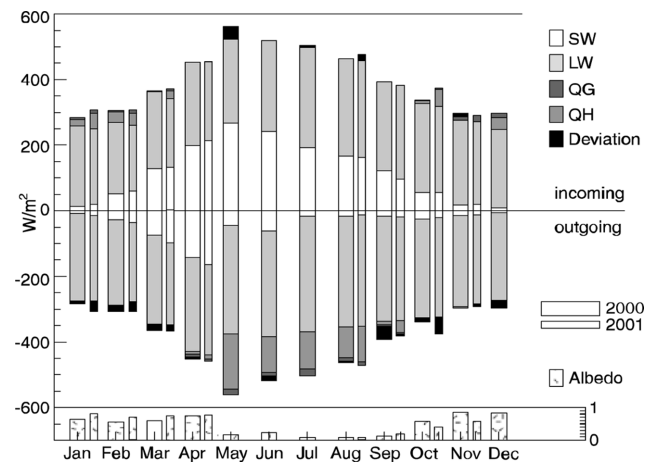


Figure 5. Energy balance components at Juvvasshøe for years 2000 and 2001. SW down, SW up, Shortwave incoming and reflected radiation; LW down, LW up, Longwave incoming and reflected radiation; Q_H sensible heat flux; Q_G ground-heat flux. Albedo is monthly averaged surface albedo, indicates if the surface is snow covered or not.

correlation on Juvvasshøe is due to high turbulent fluxes, giving good ventilation in the upper surface layer, together with small seasonal differences in thermal diffusivity. A preserved climate signal – without any high influence of other variables, such as variations in snow cover and latent heat related to phase

change – makes Juvvasshøe suited for climate and ground-surface temperature reconstruction studies.

5 CONCLUSIONS

On Juvvasshøe, net radiation and sensible heat fluxes are the dominating energy fluxes and give a near zero energy budget. There is a close relation between air-, ground surface- and ground temperatures at the study site. This relationship is mainly explained by high turbulent fluxes giving good ventilation in the upper surface layer, and by low water content, lack of vegetation and almost absent snow cover at the study site. The close relation of permafrost and ground surface temperatures forms a good base of using the Juvvasshøe permafrost-data for climate and climate changes issues. The results are a step towards future spatial modelling of the energy balance in mountain permafrost areas.

ACKNOWLEDGEMENTS

This study is based on parts of the EU project PACE (Harris et al., 2001; Sollid et al., 2000). The studies at Juvvasshøe were financed by EU, the Norwegian Research Council, the Norwegian Meteorological Institute, the Norwegian Geotechnical Institute and the Department of Physical Geography, University of Oslo. Dr Martin Hoelzle (University of Zurich) and two referees gave advice and constructive comments. The authors extend their thanks to the persons, PACE partners and to the financial resources mentioned above.

REFERENCES

- Carslaw, H.S. & Jaeger, J.C., 1959. *Conduction of heat in solids*. Oxford, Clarendon Press.
- Etzelmüller, B., Berthling, I. & Sollid, J.L., 1998. The distribution of permafrost in Southern Norway; a GIS approach. In: A.G. Lewkowicz & M. Allard (Editors), *Proceedings of the 7th International Conference on Permafrost*. Collection Nordicana. Centre d'Etudes Nordiques, Université Laval, Yellowknife Canada, pp. 251–257.
- Goodrich, L.E., 1982. The influence of snow on the ground thermal regime. *Canadian Geotechnical Journal*, 19: 421–432.
- Harris, C., Haeberli, W., Vonder Mühl, D. & King, L., 2001. Permafrost Monitoring in the High Mountains of Europe: the PACE Project in its Global Context. *Permafrost and Periglacial Processes*, 12(1): 3–11.
- Harris, S.A. & Pedersen, D.E., 1998. Thermal regimes beneath coarse blocky materials. *Permafrost and Periglacial Processes*, 9: 107–120.
- Hoelzle, M., Mittaz, C., Etzelmüller, B. & Haeberli, W., 2001. Surface Energy Fluxes and Distribution Models of Permafrost in European Mountain Areas: an Overview of Current Developments. *Permafrost and Periglacial Processes*, 12: 53–68.
- Humlum, O., 1997. Active layer thermal regime at three rock glaciers in Greenland. *Permafrost and Periglacial Processes*, 8: 383–408.
- Isaksen, I., Hauck, C., Gudevang, E., Ødegård, R.S. & Sollid, J.L., 2002. Mountain permafrost distribution on Dovrefjell and Jotunheimen, southern Norway, based on BTS and DC resistivity tomography data. *Norsk Geografisk Tidsskrift*, 56(2): 122–136.
- Isaksen, I., Vonder Mühl, D., Gubler, H., Kohl, T. & Sollid, J.L., 2000. Ground surface-temperature reconstruction based on data from a deep borehole in permafrost at Janssonhaugen, Svalbard. *Annals of Glaciology*, 31: 287–294.
- Isaksen, K., Holmlund, P., Sollid, J.L. & Harris, C., 2001. Three Deep Alpine-Permafrost Boreholes in Svalbard and Scandinavia. *Permafrost and Periglacial Processes*, 12(1): 13–25.
- King, L., 1984. Permafrost in Skandinavien. Untersuchungsergebnisse aus Lappland, Jotunheimen und Dovre/Rondane. *Heidelberger Geographische Arbeiten*, 76: 174.
- Mittaz, C., Hoelzle, M. & Haeberli, W., 2000. First results and interpretation of energy-flux measurements over Alpine permafrost. *Annals of Glaciology*, 31: 275–280.
- Mittaz, C., Imhof, M., Hoelzle, M. & Haeberli, W., 2002. Snowmelt evolution mapping using an energy balance approach over an alpine terrain. *Arctic, Antarctic and alpine Research*, 34(3): 274–281.
- Ødegård, R.S., Hoelzle, M., Johansen, K.V. & Sollid, J.L., 1996. Permafrost mapping and prospecting in southern Norway. *Norsk geografisk Tidsskrift*, 50: 41–54.
- Ødegård, R.S., Isaksen, K., Mastervik, M., Billdal, L., Engler, M. & Sollid, J.L., 1999. Comparison of BTS and Landsat TM data from Jotunheimen, southern Norway. *Norsk Geografisk Tidsskrift*, 53: 226–233.
- Ødegård, R.S., Sollid, J.L. & Liestøl, O., 1992. Ground temperature measurements in mountain permafrost, Jotunheimen, southern Norway. *Permafrost and Periglacial Processes*, 3: 231–234.
- Oke, T.R., 1987. *Boundary layer climates*. Second edition. Methuen., London.
- Østrem, G., Dale Selvig, K. & Tandberg, K., 1988. Atlas over breer i Sør-Norge. 61, The Norwegian Water Resources and Energy Directorate (NVE), Hydrology department.
- Sollid, J.L., Holmlund, P., Isaksen, K. & Harris, C., 2000. Deep permafrost boreholes in western Svalbard, northern Sweden and southern Norway. *Norsk Geografisk Tidsskrift*, 54: 186–191.
- Vonder Mühl, D. & Haeberli, W., 1990. Thermal characteristics of the permafrost within an active rock glacier (Murtèl/Corvatsch, Grisons, Swiss Alps). *Journal of Glaciology*, 36(123): 151–158.
- Zhang, T., Barry, R.G. & Haeberli, W., 2000. Numerical simulations of the influence of the seasonal snow cover on the occurrence of permafrost at high latitudes. *Norsk Geografisk Tidsskrift*, 55: 261–266.